Article

Clinical, ultrasonographic, and pathologic findings in 70 camels *(Camelus dromedarius)* with Johne's disease

Mohamed Tharwat, Fahd Al-Sobayil, Ahmed Ali, Mahmoud Hashad, Sébastien Buczinski

Abstract — This study evaluated the use of ultrasonography for the diagnosis of Johne's disease in camels *(Camelus dromedarius)*. Seventy camels with confirmed Johne's disease were examined by ultrasonography and subsequent necropsy; 15 healthy camels were included as controls. The most outstanding findings were visible enlargement of the mesenteric lymph nodes in 52 (74%) camels. Lesions had either echogenic (26%; *n* = 18) or anechoic (69%; *n* = 48) capsule and the contents were either anechoic (21%; *n* = 15), echogenic (27%; *n* = 19), or heterogeneous (46%; *n* = 32). Clumps of echogenic tissue interspersed with fluid pockets were imaged between the intestinal loops in 9 (13%) camels. There was mild, moderate, or severe thickening and corrugation of the intestinal wall, excessive anechoic fluid in the abdominal cavity in 18 (26%) camels, increased hepatic brightness in 30 (43%) camels, and pericardial and pleural effusions in 22 (31%) camels. Sensitivity values for detecting intestinal lesions and enlarged mesenteric lymph nodes were 95% and 84%, respectively.

Résumé — Constatations cliniques, échographiques et pathologiques chez 70 chameaux *(Camelus dromedarius)* atteints de la maladie de Johne. Cette étude a évalué l'usage de l'échographie pour le diagnostic de la maladie de Johne chez les chameaux *(Camelus dromedarius)*. Soixante-dix chameaux chez lesquels la maladie de Johne avait été confirmée ont été examinés par échographie et nécropsie subséquente; 15 chameaux en santé ont été inclus comme témoins. Les constatations les plus exceptionnelles étaient une augmentation visible de la taille des ganglions lymphatiques mésentériques chez 52 (74 %) chameaux. Les lésions présentaient soit des capsules échogènes (26 %; *n* = 18) ou anéchogènes (69 %; *n* = 48) et le contenu était soit anéchogène (21 %; *n* = 15), échogène (27 %; *n* = 19) ou hétérogène (46 %; *n* = 32). Des grappes de tissu échogène parsemées de poches de liquide ont été imagées entre les boucles intestinales chez 9 (13 %) chameaux. Il y avait un épaississement ou une corrugation d'un stade léger, modéré ou sévère de la paroi intestinale, une quantité excessive de liquide anéchogène dans la cavité abdominale chez 18 (26 %) chameaux, une luminosité hépatique accrue chez 30 (43 %) chameaux et des effusions péricardiques et pleurales chez 22 (31 %) chameaux. Les valeurs de sensibilité pour détecter les lésions intestinales et les ganglions lymphatiques mésentériques hypertrophiés étaient de 95 % et de 84 %, respectivement.

(Traduit par Isabelle Vallières)

Can Vet J 2012;53:543–548

Introduction

Johne's disease or paratuberculosis is characterized by persistent and progressive diarrhea, weight loss, debilitation, and eventual death. The disease occurs worldwide and affects cattle, sheep, goats, camels, farmed deer, and other domestic and wild ruminants (1,2). In tropical areas with intensive camel farming, paratuberculosis presents a serious economic problem due to culling of animals, reduced milk production, and the costs of laboratory testing and control measures (3). In Saudi Arabia, camel's milk, with or without pasteurization, is consumed heavily by local humans. As the causative organism, *Mycobacterium avium* subsp. *paratuberculosis* (MAP), may also be a cause of Crohn's disease in humans (4,5), milk from infected animals may be hazardous to the health of consumers.

Although the organisms can be shed in milk, the fecal-oral route is the primary mechanism for transmission of MAP and this is reflected in disease control recommendations (6). These are mainly based on removal of animals with clinical signs,

Department of Veterinary Medicine, College of Agriculture and Veterinary Medicine, Qassim University, Saudi Arabia (Tharwat, Al-Sobayil, Ali, Hashad); Bovine Ambulatory Clinic, Departement des Sciences Cliniques, Faculté de Médecine Vétérinaire, Université de Montréal, Saint-Hyacinthe, Quebec, Canada (Buczinski).

Dr. Tharwat's permanent address is Department of Animal Medicine, Faculty of Veterinary Medicine, Zagazig University, Egypt.

Address all correspondence to Dr. Sébastien Buczinski; e-mail: s.buczinski@umontreal.ca

identification of subclinical cases by testing, and feeding MAP-free colostrum and milk to neonatal animals (7,8). Definitive diagnosis of Johne's disease is based on culture and identification of MAP from feces or tissue. The organism is slow growing, requiring 4 to 16 wk and special growth media. Other diagnostic tests used to screen herds and make a diagnosis in individual livestock species include agar gel immunodiffusion (AGID), complement fixation, competitive enzyme-linked immunosorbent assay (ELISA), histologic pattern of a granulomatous reaction, Ziehl-Neelsen staining (acid-fast) of tissue and feces, polymerase chain reaction (PCR), and DNA probes (3,9).

In dogs, transabdominal ultrasonography is a widely used ancillary test for assessment of patients with chronic intestinal inflammation. Despite its low sensitivity, it has reportedly been used for testing chronic inflammatory bowel syndrome in which severe intestinal thickening is observed (10). In addition, ultrasonography of the intestine in cats with inflammatory bowel disease (IBD), showed several abnormalities (such as poor intestinal wall layer definition, focal thickening), and large mesenteric lymph nodes with hypoechoic changes appearing to have the best association with histologic grade of IBD (11).

The present study was carried out to determine the clinical, ultrasonographic, and pathologic findings in dromedary camels with Johne's disease as a step toward establishing a rapid, field diagnostic tool for early detection and culling of diseased camels. To the authors' knowledge, this is the first study to document ultrasonographic findings in camels *(Camelus dromedarius)* suffering from Johne's disease.

Materials and methods

Animals, history and physical examination

Camels referred to the Veterinary Teaching Hospital, Qassim University, from various herds in the central region of Saudi Arabia between 2007 and 2011 were used for the study. Of these (n = 70) diseased female Arabian camels *(Camelus dromedarius)* (mean age: 2.3 ± 1.0 y), 17 were pregnant and 31 were lactating. The duration of illness ranged from 1 wk to 12 mo, and the camels had been treated with various medications by field veterinarians, including oral and systemic antibiotics, corticosteroids, and anthelmintics. Fifteen apparently healthy female Arabian camels (mean age: 2.5 ± 1.1 y) were included in the study as controls. Both diseased and control camels underwent a thorough physical examination (12), including general behavior and condition, auscultation of the heart, lungs, rumen and intestine, detection of heart and respiratory rates, and rectal temperature. Based on a 1 to 5 scale, the body condition score (BCS) of control and diseased camels was determined using a previously described protocol (13). Inclusion criteria for diseased camels included PCR-positive fecal samples for paratuberculosis. Control camels were categorized as healthy based on PCR-negative results for paratuberculosis and normal physical and ultrasonographic examination.

Hematological and biochemical analyses

Two blood samples were collected from the jugular vein of each control and diseased camel upon admission. One sample was collected into EDTA-containing tubes for hematological tests. The other sample was collected in plain tubes to obtain serum for biochemical parameters. Hematological examination (hematocrit, hemoglobin, total leucocyte count) was carried out using an automated veterinary analyzer (Vet Scan HM5; ABAXIS, Budapest, Hungary). For serum samples, commercial kits (Human Gesellschaft fur Biochemica und Diagnostica, Wiesbaden — Germany) were used (14). The concentrations of total protein, calcium, phosphorus, magnesium, glucose, total bilirubin, blood urea nitrogen (BUN), and creatinine in serum were determined. The activities of aspartate aminotransferase (AST) and γ-glutamyl transferase (GGT) were also tested in serum samples. An automated biochemical analyzer (Biosystems A15, Spain) was used for measurement of all serum parameters. Rectal smears and fecal samples were collected from all diseased camels and also from control animals for Ziehl-Neelsen staining and PCR.

Ultrasonographic examination

Ultrasonographic examination was carried out on control and diseased camels while the animals were recumbent, using 3.5 and 5.0 MHz sector and linear transducers (SSD-500; Aloka, Tokyo, Japan). Animals were slightly sedated using xylazine (Bomazine 10%; Bomac Laboratories, Auckland, New Zealand), 0.3 mg/kg body weight (BW), IV. The skin was shaved on both sides of the abdomen and thorax. After the application of transmission gel to the transducer, the animals were examined beginning at the caudal abdomen and extending forward to the third intercostal space on both sides of the thorax. Each intercostal space was examined dorsoventrally, with the transducer held parallel to the ribs. In the abdomen, the peritoneum, stomachs, spleen, small and large intestines, liver, pancreas, and kidneys were imaged. In the thoracic cavity, the lungs, heart and its major blood vessels and the mediastinal region were scanned. During ultrasonography of the abdomen, small intestinal wall thickness was measured in each camel for 3 intestinal loops using ultrasound calipers, and the mean value was determined. Mesenteric lymph node enlargement was measured in a similar pattern. For detecting the sensitivity of transabdominal ultrasound in the antemortem diagnosis of intestinal wall thickening and corrugation and enlargement of mesenteric lymph nodes, the diseased camels were euthanized and a thorough postmortem examination was performed.

DNA extraction and polymerase chain reaction

To prepare genomic DNA templates from camel tissues and feces, about 0.5 g of feces or lymph node tissue was homogenized in 5 mL normal saline and boiled in a water bath for 10 min. Samples were centrifuged at 200 × g for 30 s, and 0.5 mL of the supernatant from each sample was transferred to new 15 mL conical tubes and mixed with an equal volume of lysis buffer [2% Triton X-100, 1% sodium dodecyl sulfate, 100 mM NaCl, 10 mM Tris-HCl, (pH 8.0)]. After addition of 10 μL of proteinase K (stock 10 mg/mL distilled water) to each mixture, the tubes were incubated at 65°C for 1 h (15). Genomic DNA was obtained using a phenol extraction method developed in the laboratory (16).

Reaction tubes contained a total volume of 25 μL consisting of ultrapure distilled water (DNAase, RNAase-free), 2.5 μL

Table 1. Hematological and biochemical findings [median (1st–3rd quartiles)] in camels with Johne's disease compared to controls ([a]$P < 0.05$; [b]$P < 0.01$)

Parameters	Finding at admission ($n = 70$)	Controls ($n = 15$)
Hematocrit (%)	16 (14–18)[b]	34 (30.4–34.0)
Hemoglobin (g/L)	70 (60–68)[a]	110 (85–140)
Leukocyte count $\times 10^3$ (/μL)	23.3 (29.3–39.8)[b]	8.6 (8.0–14.1)
Total protein (g/L)	49 (36–53)[b]	79 (75–82)
Albumin (g/L)	21 (17–24)[b]	43 (35–50)
Globulin (g/L)	28 (19–34)[b]	36 (24–47)
Aspartate aminotransferase (U/L)	251 (155–274)[b]	75 (35–114)
γ-glutamyl transferase (U/L)	43 (29–70)	38 (19–60)
Total bilirubin (μmol/L)	8.6 (8.6–8.6)	10.3 (3.4–17.1)
Urea nitrogen (mmol/L)	12.5 (8.0–15.7)	7.9 (3.6–12.5)
Creatinine (mmol/L)	123.8 (132.6–141.4)	114.9 (61.9–141.4)
Calcium (mmol/L)	4 (1.8–2.3)	2.8 (2.0–2.2)
Phosphorus (mmol/L)	1.6 (1.2–1.9)	2.0 (1.9–2.4)
Magnesium (mg/dL)	0.62 (0.37–0.86)[b]	0.99 (0.99–1.0)
Glucose (mg/dL)	1.9 (1.4–3.1)[b]	3.9 (3.6–4.2)

Table 2. Ultrasonographic findings in 70 camels with Johne's disease

Findings	(%) Number
Severe thickening and corrugation of the small intestinal mucosa	59 (84)
Visible enlargement of the mesenteric lymph nodes	52 (74)
Enlarged lymph nodes with anechoic capsule	48 (69)
Enlarged lymph nodes with heterogeneous capsule	32 (46)
Increased hepatic brightness	30 (43)
Pericardial and pleural effusions	22 (31)
Enlarged lymph nodes with echogenic contents	19 (27)
Accumulation of anechoic fluid in the abdominal cavity	18 (26)
Enlarged lymph nodes with echogenic capsule	18 (26)
Enlarged lymph nodes with anechoic contents	15 (21)
Presence of clumps of echogenic tissue interspersed with fluid pockets between the intestinal loops	9 (13)
Moderate thickening and corrugation of the small intestinal mucosa	8 (11)
Mild thickening and corrugation of the small intestinal mucosa	3 (4)

of 10× PCR buffer, 2.5 mM $MgCl_2$, 0.25 mM deoxyribonucleoside triphosphates, 0.25 mM primers, and 1.5 U of *Taq* polymerase. Primer sequences for the MAP–specific genetic element, IS900, were used in the reaction mixture as follows: 5′-CCGCTAATTGAGAGATGCGATTGG-3′, forward primer, and 5′-AATCAACTCCAGCAGCGCGGCCTCG-3′, backward primer, to amplify a 229-bp gene sequence. Samples were run according to this protocol: 1 cycle at 94°C for 10 min; 50 cycles at 94°C for 59 s, 60°C for 30 s, and 72°C for 59 s; followed by a final extension at 72°C for 10 min. The PCR product was electrophoresed in 1% agarose in 1× tris-acetic acid-EDTA (TAE) buffer with ethidium bromide (1 μg/mL) covered with 1× TAE buffer (16). The DNA bands were visualized on a UV transilluminator (Foto/Phoresis, Fotodyne Incorporated, Hartland, Wisconsin, USA) and the gel was photographed using a digital camera (Canon, Japan).

Statistical analysis

Data are presented as medians with 1st (25%) and 3rd (75%) quartiles and the analysis was conducted using SPSS program (18). Hematological and biochemical data were compared between diseased and control camels, using the Mann-Whitney U-test. The level of significance was set at $P < 0.05$.

Results

Clinical and biochemical findings

Compared to a BCS of 3.5 ± 0.6 in control camels, the BCS in diseased camels were 2.4 ± 0.5 in 25 (36%) camels and 1.4 ± 0.4 in 45 (64%) camels. The most prominent clinical signs in the diseased camels were chronic intermittent diarrhea in 67 (96%) camels, inappetance in all cases (100%), and weak and irregular ruminal contractions in 53 (76%) camels. Six camels (9%) had attacks of abdominal pain after admission. Hematological and biochemical findings are summarized in Table 1. Compared to controls, results from diseased camels showed low packed cell volume in 65 camels ($P < 0.01$), leukocytosis in 54 ($P < 0.01$), decreased hemoglobin in 37 ($P < 0.05$), hypoproteinemia with hypoalbuminemia and hypoglobulinemia in 50 ($P < 0.01$), hypoglycemia in 42 ($P < 0.01$), hypomagnesemia in 19 ($P < 0.01$), and increased serum activity of AST in 34 camels ($P < 0.01$). The serum activity of GGT as well as the concentrations of total bilirubin, BUN, creatinine, phosphorus, and calcium did not differ significantly compared with controls. Rectal smears stained with Ziehl-Neelsen method showed acid-fast bacilli in all diseased camels and were negative in all controls.

Ultrasonographic findings

Table 2 summarizes the ultrasonographic findings in the camels with Johne's disease. Compared with the intestinal wall thickness in control camels that measured 3.6 ± 1.2 mm, mild (6.8 ± 1.9 mm), moderate (12.8 ± 4.6 mm), and severe (17.5 ± 3.6 mm) thickening and corrugation of the small intestinal wall was imaged in the camels with Johne's disease (Figure 1). The mesenteric lymph nodes were not detected on ultrasonographs of the control camels. However, in the diseased camels, the most outstanding sonographic finding was the enlargement of mesenteric lymph nodes that was confirmed at necropsy. Enlarged lymph nodes had either echogenic or anechoic capsule, and anechoic, echogenic or heterogeneous contents (Figure 2). Clumps of echogenic tissue interspersed with fluid pockets were imaged between the intestinal loops in 9 camels (Figure 3). Compared to healthy controls, hepatic ultrasonographs showed an overall increased brightness in 30 camels (Figure 4). Pericardial and pleural effusions were imaged as an anechoic fluid in 22 camels. No detectable scanning abnormalities were observed while imaging stomachs, spleen, pancreas, and kidneys.

Necropsy and polymerase chain reaction findings

Only the diseased camels were subjected to euthanasia and postmortem examination. Diffuse thickening and corrugation of the small intestine was seen in 65 camels. In these cases, the mucous membranes were increased in size, forming folds (Figure 5). Ulceration of the large intestine with hemorrhages was seen in 13 animals and a folded mucosa was observed in 22 camels. The mesenteric lymph nodes were highly swollen in

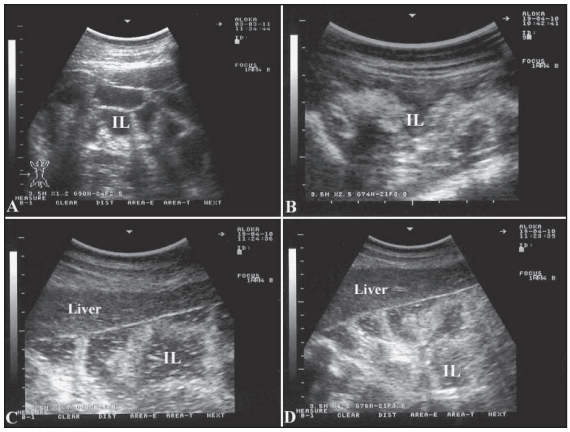

Figure 1. Ultrasonographic appearance of the intestines in a healthy camel (A) and in 3 diseased camels (B, C, D) with Johne's disease. Excessive accumulation of anechoic fluid, moderate to severe thickening and corrugation of the intestinal mucosa are apparent in sick animals. Images were taken at the right ventral abdomen using a 3.5 MH sector transducer. IL – intestinal loops.

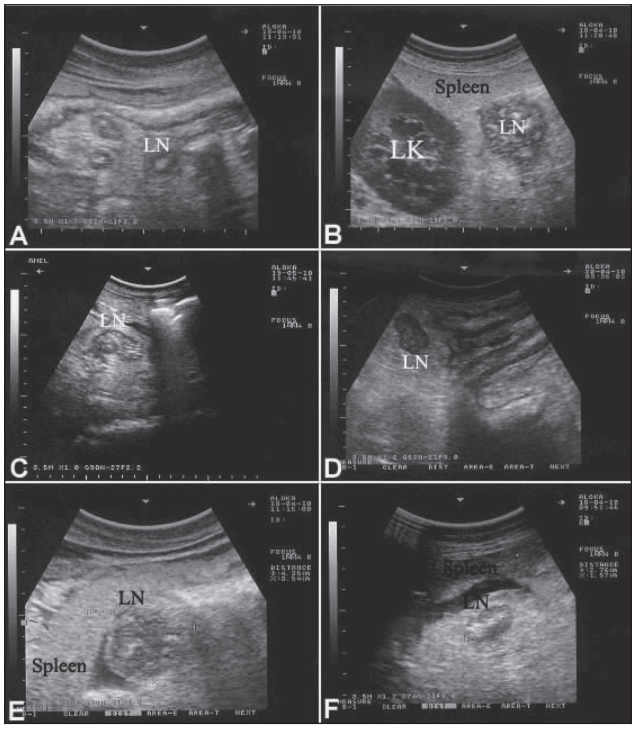

Figure 2. Ultrasonographic appearance of enlarged mesenteric lymph nodes in 6 camels with Johne's disease. Enlarged lymph nodes in A, B, C, D and F had a well-developed anechoic capsule; the contents are echogenic in A and F, heterogeneous in B and C and anechoic in D. In image E, the capsule is echogenic and the content is heterogeneous. Images were taken at the right (A, C, D) and left (B, E, F) ventral abdomen using a 3.5 MH sector transducer. LN – lymph node; LK – left kidney.

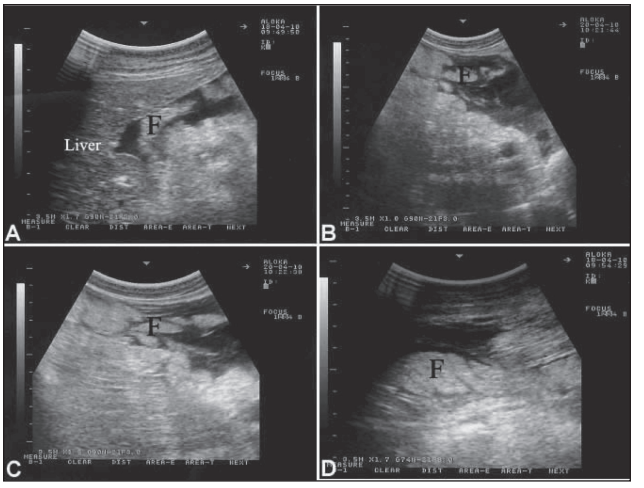

Figure 3. Ultrasonographic appearance of the abdomen in 4 camels with Johne's disease. In A, B, C and D, clumps of echogenic tissue (F) interspersed with fluid pockets were imaged between the intestinal loops. Images were taken at the right ventral abdomen using a 3.5 MH sector transducer.

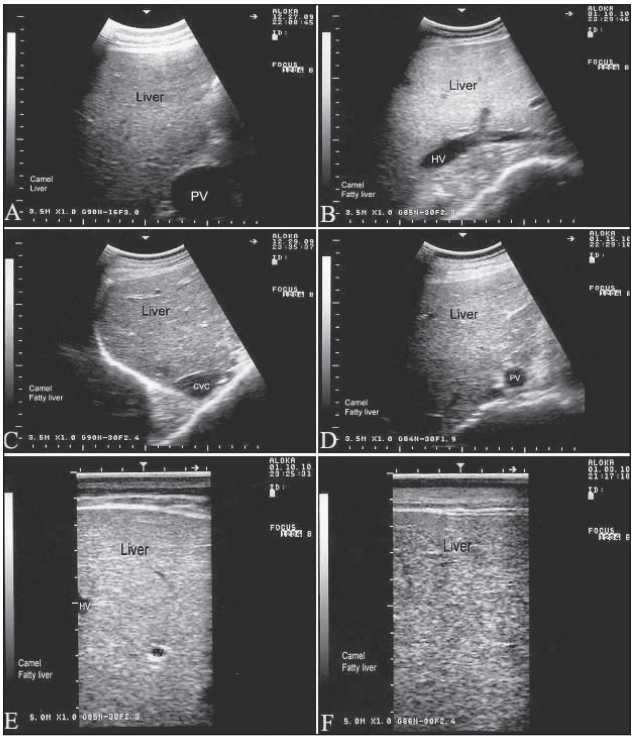

Figures 4. Ultrasonographs in 5 camels with Johne's disease. Images were taken from the 11th intercostal space on the right side. Compared to healthy animal (A), the liver appears hyperechogenic on ultrasonographs (B, C, D, E, F). PV – portal vein; HV – hepatic vein; CVC – caudal vena cava.

62 camels; 43 of them were hemorrhagic on cut section. The hepatic lymph nodes were also enlarged in 6 camels. Other postmortem findings included fatty infiltration of the liver in 33 camels, and pleural, pericardial, and peritoneal effusions in 24 camels (Figure 6). The DNA extracted from rectal samples and lymph nodes of paratuberculosis-suspected cases, according to ultrasonography and Ziehl-Neelsen staining, resulted in amplification of a 229-bp PCR product which is the expected product of MAP-*IS900*. Samples obtained from controls, however, did not show a PCR product of the predicted size.

Discussion

Paratuberculosis is known to cause intestinal and hepatic lesions in sheep, goats, cattle, and camels (19–21), but it remains a

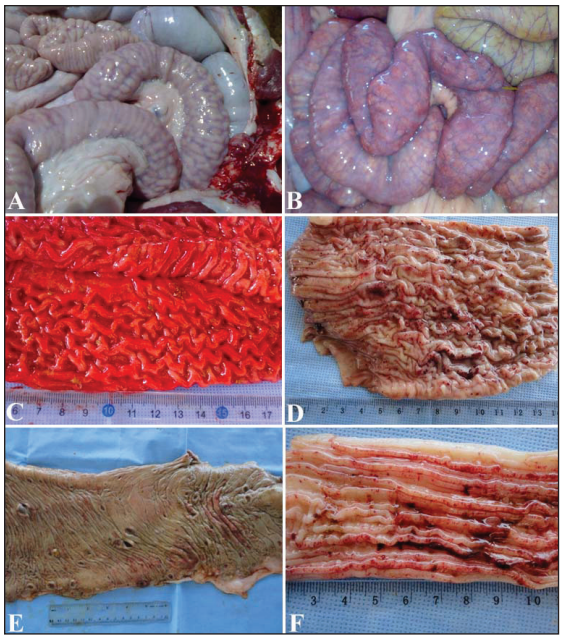

Figure 5. Postmortem findings in 6 camels with Johne's disease. Intestinal mucous membrane showed thickening, corrugation (A, B, C, D) and ulceration and hemorrhages (D, E, F).

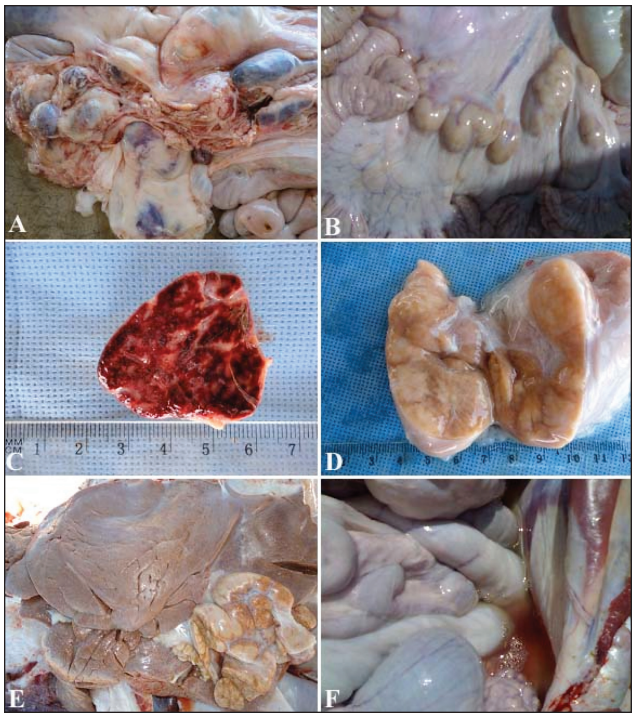

Figure 6. Postmortem findings in 3 camels with Johne's disease. Images A and B show enlargement of the mesenteric lymph nodes that on cut section were hemorrhagic in C or with granulomas and abscesses in D. Image E shows enlargement and granulomas of the hepatic lymph node. Additional necropsy findings included peritoneal effusions (F).

significant problem to the researcher, field diagnostician, and animal producers (1,3). The lack of diagnostic tools that can be directly used on farm is an impediment to control programs. Transabdominal ultrasonography is a non-invasive diagnostic tool that is increasingly being used in ruminant medicine and surgery. It can also be used to assess the small and large intestine in cattle (22,23). The present study was therefore designed to determine the ultrasonographic findings in camels with Johne's disease as a step toward establishing a rapid field diagnostic tool for detection and removal of infected animals.

In the present study, Johne's disease was suspected in camels that exhibited chronic loss of body condition and/or chronic or intermittent diarrhea that did not respond to treatment. Diarrhea may explain the reduced hematocrit value and increased magnesium concentration. Hypoproteinemia, hypoalbuminemia, and hypoglobulinemia could all be attributed to the malabsorption diarrhea. Other factors such as reduced appetite and emaciation as the disease progressed may have contributed to changes in these serum parameters. Leukocytosis could be explained by the chronic nature of the disease. Research efforts have been concentrated on mechanisms of disease transmission, factors influencing susceptibility, serologic identification of carrier animals, and other means of early diagnosis (3).

No data are available concerning ultrasonography as a diagnostic aid in the diagnosis of paratuberculosis in ruminants. In this study, there was a significant difference in intestinal wall thickness between normal and diseased camels and enlarged mesenteric lymph nodes could only be imaged in clinically affected camels. These data may be useful for clinicians in the field. Ultrasound detection of intestinal corrugation in camels with Johne's disease was successful in 95% of the cases. Similarly, ultrasound was effective in detecting enlarged mesenteric lymph nodes in 84% of the diseased camels. In the 16% of cases in which enlarged mesenteric lymph nodes could not be imaged antemortem, this could be due to the enlarged lymph nodes being beyond the depth of the ultrasound beam. Ultrasonography was also useful in imaging clumps of echogenic tissue interspersed with fluid between the intestinal loops, reflecting the chronicity of the disease.

A diagnostic PCR test based on specific DNA sequences in the MAP genome allowed fast and accurate identification of this slow-growing bacterium. The PCR results confirmed the presence of MAP in the animals suspected of having Johne's disease and, along with the observations at necropsy, allowed ultrasonographic findings to be related to Johne's disease. The PCR has been used to confirm positive culture results and to identify MAP in feces, milk, and tissues (24,25). Although some authors found sensitivities varying from 3% to 23% in comparison to culture (26), others obtained a sensitivity of 94.1%, using the freeze-boiling extraction methodology for DNA isolation (27). Results obtained with PCR carried out in the present study coincide with the high sensitivity and specificity of the test and there were no problems related to inhibitory substances in the fecal samples.

In conclusion, ultrasonographic examination of camels with suspected Johne's disease can be helpful in screening animals waiting for confirmation by definitive tests (culture, ELISA, or PCR). The procedure was especially valuable in determining macroscopic intestinal lesions as well as enlargement of the mesenteric lymph nodes that reflected the severity of the

inflammatory changes, which were confirmed at postmortem examination.

Acknowledgments

The authors thank the referring veterinary practitioners and farmers for contributing cases. Appreciation is extended to Dr. N. Peachy (Professor of English), Qassim University, for assisting with English language use. This study was supported by the Deanship for Scientific Research (SR-D-011-602), Qassim University, Saudi Arabia. CVJ

References

1. Radostits OM, Gay CC, Hinchcliff KW, Constable PD. Veterinary Medicine. A Textbook of the Diseases of Cattle, Sheep, Pigs, Goats and Horses. 10th ed., St. Louis, Missouri: Saunders-Elsevier, 2007.
2. Wernery U, Kaaden OR. Infectious Diseases in Camelids. Berlin, Germany: Blackwell Science, 2002:83–90.
3. Fowler ME. Medicine and Surgery of Camelids. 3rd ed. Ames, Iowa: Blackwell Publishing, 2010:204–207.
4. Stott AW, Jones GM, Humphry RW, Gunn GJ. Financial incentive to control paratuberculosis (Johne's disease) on dairy farms in the United Kingdom. Vet Rec 2005;156:825–831.
5. Chamberlin WM, Naser SA. Integrating theories of the etiology of Crohn's disease. On the etiology of Crohn's disease: Questioning the hypotheses. Med Sci Monitor 2006;12:RA27–RA33.
6. Clarke CJ. The pathology and pathogenesis of paratuberculosis in ruminants and other species. J Comp Pathol 1997;116:217–261.
7. Kennedy DJ, Benedictus G. Control of *Mycobacterium avium* subsp. *paratuberculosis* infection in agricultural species [Review]. Revue Scientifique et Technique Office international des épizooties 2001; 20:151–179.
8. Benedictus G, Kalis CJH. Paratuberculosis: Eradication, control and diagnostic methods. Acta Vet Scand 2003;44:231–241.
9. Ellingson JLE, Koziczkowski JJ, Anderson JL. Comparison of PCR prescreening to two cultivation procedures with PCR confirmation for detection of *Mycobacterium avium* subsp. *paratuberculosis* in U.S. Department of Agriculture fecal check test samples. J Food Protect 2004;67:2310–2314.
10. Rudorf H, van Schaik G, O'Brien RT, Brown PJ, Barr FJ, Hall EJ. Ultrasonographic evaluation of the thickness of the small intestinal wall in dogs with inflammatory bowel disease. J Small Anim Pract 2005;46:315–316.
11. Baez JL, Hendrick MJ, Walker LM, Washabau RJ. Radiographic, ultrasonographic, and endoscopic findings in cats with inflammatory bowel disease of the stomach and small intestine: 33 cases (1990–1997). J Am Vet Med Assoc 1999;215:349–354.
12. Köhler-Rollefson I, Mundy P, Mathias E. A Field Manual of Camel Diseases: Traditional and Modern Healthcare for the Dromedary. London, England: ITDG publishing, 2001:1–67.
13. Sghiri A, Driancourt MA. Seasonal effects on fertility and ovarian follicular growth and maturation in camels *(Camelus dromedarius)*. Anim Reprod Sci 1999;55:223–237.
14. Ali A, Tharwat M, Al-Sobayil FA. Hormonal, biochemical, and hematological profiles in female camels *(Camelus dromedarius)* affected with reproductive disorders. Anim Reprod Sci 2010;118:372–376.
15. Bosshard C. *Mycobacterium avium* subsp. *paratuberculosis* prevalence studies in bulk tank raw milk and slaughtered healthy dairy cows in Switzerland using an F57 sequence-based real-time PCR assay. PhD thesis, 2006, Institut für Lebensmittelsicherheit und — hygiene der Vetsuisse-Fakultät Universität Zürich.
16. Ilhan Z, Solmaz H, Aksakal A, Gulhan T, Ekin IH, Boynukara B. Detection of *Brucella melitensis* DNA in the milk of sheep after abortion by PCR assay. Arch Med Vet 2008;40:141–146.
17. Stabel JR, Bosworth TL, Kirkbride TA, Forde LR, Whitlock RH. A simple, rapid, and effective method for the extraction of *Mycobacterium paratuberculosis* DNA from fecal samples for polymerase chain reaction J Vet Diagn Invest 2004;16:22–30.
18. SPSS. Statistical Package for Social Sciences, SPSS Inc., Chicago, Illinois, USA Copyright© for Windows, version 16.0; 2007.
19. Jones TC, Hunt RD, King NW. Paratuberculosis. In: Veterinary Pathology. 6th ed. Baltimore, Maryland: Williams and Wilkins, 1997: 498–501.
20. Radwan AI, El-Magawry S, Hawari A, Al-Bekairi SJ, Aziz S, Rebleza RM. Paratuberculosis enteritis (Johne's disease) in camels in Saudi Arabia. Biol Sci 1991;1:57–66.
21. Mahmoud OM, Haroun EM, Elfaki MG, Abbas B. Pigmented paratuberculosis granulomata in the liver of sheep. Small Rumin Res 2002;43: 211–217.
22. Braun U, Marmier O. Ultrasonographic examination of the small intestine of cows. Vet Rec 1995;136:239–244.
23. Braun U, Amrein E. Ultrasonographic examination of the caecum and the proximal and spiral ansa of the colon of cattle. Vet Rec 2001;149: 45–48.
24. Coussens PM. Model for immune responses to *Mycobacterium avium* subspecies *paratuberculosis* in cattle. Infect Immun 2004;72:3089–3096.
25. Paustian ML, Amonsin A, Kapur V, Bannantinne J. Characterization of novel coding sequences specific to *Mycobacterium avium paratuberculosis:* Implications to diagnosis of Johne's Disease. J Clin Microbiol 2004; 42:2675–2681.
26. Waters WR, Stabel R, Sacco RE, Harp JÁ, Pesch BA, Wannemuehler MJ. Antigen specific B-cell unresponsiveness induced by chronic *Mycobacterium paratuberculosis* infection of cattle. Infect Immun 1999;67: 1593–1598.
27. Garrido JM, Cortabarria N, Oguisa JA, Aduriz G, Juste RA. Use of PCR method on faecal samples for diagnosis of sheep paratuberculosis. Vet Microbiol 2000;77:339–349.